Atmósfera (2003) 257-283

On the evaluation of the representation of mid-latitude transients in the Southern Hemisphere by HadAM2B GCM and the impact of horizontal resolution

S. A. SOLMAN, M.N. NUÑEZ
CIMA (CONICET-UBA) / Dto. Cs. de la Atmósfera y los Océanos (UBA)
Ciudad Universitaria - Pabellón II - 2° Piso (1428) Buenos Aires, Argentina
P. R. ROWNTREE
Hadley Centre for Climate Prediction and Research
Meteorological Office, London Road, Bracknell,
Berkshire, RG12 2SY, UK
Corresponding author: S. A. Solman; e-mail: solman@at.fcen.uba.ar

Received August 14, 2002; accepted September 4, 2003

RESUMEN

Se presenta una evaluación del Modelo de Circulación General de la Atmósfera, HadAM2b, del Hadley Centre, con énfasis en la actividad sinóptica del Hemisferio Sur. Asimismo, se realizó una evaluación del efecto de la resolución horizontal en la calidad de la simulación. Se compararon las simulaciones realizadas para al período AMIP con el modelo de resolución estándar (2.5° de latitud por 3.75° de longitud) y de alta resolución (0.833° de latitud por 1.25° de longitud), en los cuales ambos modelos fueron forzados con la climatología observada de temperatura de superficie del mar, con los re-análisis provenientes de NCEP y ERA para el período 1979-1988. Se analizaron algunas variables representativas del estado medio climatológico y propiedades que caracterizan la actividad de escala sinóptica para el Hemisferio Sur. Los resultados obtenidos mostraron que el modelo en ambas resoluciones reproduce considerablemente bien los patrones básicos observados del campo de presión de superficie y la corriente en chorro de niveles superiores. En general, los cambios debido al aumento de la resolución no representan una mejora significativa en la calidad de la simulación. La actividad de escala sinóptica está razonablemente bien simulada, aunque sobreestimada respecto a los re-análisis de NCEP, para ambas resoluciones. Esta sobreestimación es menor respecto a los re-análisis ERA. La magnitud de la energía cinética de las perturbaciones y los flujos de calor y cantidad de movimiento en las regiones de máxima actividad sinóptica, rutas de tormentas, aumentan con la resolución, aunque algunas características regionales resultan mejor simuladas con el modelo de alta resolución. Ambos modelos capturan la estructura y evolución temporal de las perturbaciones sinópticas, aunque la amplitud de las

mismas es mayor que en los análisis. Asimismo, ambos modelos capturan la propagación norte-este de las ondas en la vecindad de la cordillera de los Andes, aunque la variación NO-SE de las perturbaciones en el lado de sotavento es ligeramente sobrestimada, en concordancia con el mayor momento de flujo de vórtice. La influencia orográfica de la cordillera de los Andes en la propagación de las ondas está bien representada. El modelo de alta resolución captura más adecuadamente el comportamiento de las ondas que emanan de la rama polar de las rutas de tormenta del Pacífico.

ABSTRACT

An evaluation of the Hadley Centre atmospheric general circulation model, HadAM2b, is presented, focusing on the ability of the model to simulate Southern Hemisphere (SH) transient disturbances. An assessment is also made of the effect of changing resolution. Standard resolution (2.5° latitude by 3.75° longitude) and high resolution (0.833° latitude by 1.25° longitude) AMIP (Atmospheric Model Intercomparison Project) runs in which the models are forced with observed monthly varying sea surface temperature (SST) are compared with NCEP and ERA re-analysis data for the period 1979-1988. We focus on the model's simulation of selected variables representative of the mean state and eddy properties which characterise synoptic-scale activity of the SH. Both models reproduce the basic observed patterns of the pressure field and upper level jetstream quite well. Overall, the changes due to increasing resolution do not represent an improvement in the simulated climate. The transient eddy activity is reasonably well simulated, though overestimated, relative to the NCEP re-analysis, at both resolutions. This overestimation is much less when compared with ERA. The magnitudes of the eddy kinetic energy, momentum fluxes and heat fluxes in the latitudes of the storm tracks increase with resolution, though some regional features are better simulated with the high-resolution model. Both models capture the structure and time evolution of synoptic-scale disturbances very well, though the amplitude of the disturbances is larger than in the analysis. Both models also capture the north-eastward propagation of the waves in the vicinity of the Andes, though the NW-SE tilt of the disturbances on the lee side are slightly overestimated, in agreement with larger eddy momentum flux. The orographic influence of the Andes mountains is better resolved in the high-resolution simulation for the waves emanating from the polar branch of the Pacific storm-track.

Key words: Southern Hemisphere, General Circulation Model, resolution, transient activity.

1. Introduction

General Circulation Models (GCMs) have become useful in diagnosing and understanding the processes associated with large-scale phenomena. Validation studies play an important role in facilitating the improvement of GCMs and they provide a perspective on the limitations of the model, which need to be taken into account when interpreting past and future climate simulations. To increase confidence in the predictions of the climate models used in the study of future climate change, it is important to validate as many aspects of the models as possible. Most of the validation studies are focused on the mean climate. However, the features of the mean climate have competing effects on the behaviour of the mid-latitude 'transients', i.e., the mid-latitude synoptic scale systems whose ensemble effect is referred to as 'storm tracks'. It has been demonstrated that these transient eddies force the stationary component (Lau and Nath, 1991; Orlanski, 1998), so it is important to simulate adequately the transient disturbances which are responsible, in part, for the mean state.

In the Southern Hemisphere (SH), synoptic-scale disturbances are responsible for a significant portion of the poleward heat and momentum transports and it is thus important to study these transient disturbances in both observed and model data.

Several features of tropospheric circulation in the SH are unique, due largely to the almost uninterrupted ocean between 35°S and 70°S. As a consequence, the circulation exhibits greater zonal symmetry than in the Northern Hemisphere (Adler, 1971; Karoly *et al.*, 1998). However, well-defined zonal asymmetries associated with standing waves exert important effects on regional climate (van Loon and Jenne, 1972; Wallace, 1983). As a consequence of the difference in climatic controls between the two hemispheres, evaluations of GCM performance for the Northern Hemisphere cannot be relied upon as indicators of equivalent performance in the SH. Unfortunately, relatively few studies have been performed that examine the hemisphere-wide performance of GCMs in the SH (Raphael, 1998; Meehl, 1998; Whetton *et al.,* 1996). Most of the articles examine the global performance of the GCMs (Hurrell *et al.,* 1998; Stratton, 1999).

However, several assessments of the simulation of regional circulation features by GCMs in the SH are available; we can cite Whetton *et al.* (1994), Joubert (1997), Katzfey and McInnes (1996) and Hudson and Hewitson (1997).

Some of the features of the SH circulation that are commonly not well reproduced by many GCMs are the intensity of the polar trough, the split of the westerly jet during the winter season and the intensities and locations of the storm tracks. Hurrell *et al.* (1998) in their evaluation of CCM3 GCM have found the simulated circumpolar Antarctic trough to be too deep throughout the year, westerlies too strong during both summer and winter and the double jet structure during winter season not well captured by the model. Consistent with these shortcomings CCM3 fails to reproduce some regional features in the eddy kinetic energy field and the poleward transient heat and momentum fluxes, though many of the mean features are well simulated.

Most of the GCMs used for long climate integrations use relatively coarse resolutions (grid length larger than 2.5°) which cannot accurately resolve synoptic scale weather systems. However, it has been demonstrated that most of the systematic errors in climate models (those in mean winds, temperature, heights and mean sea level pressure) appear to be almost independent of resolution (Boville 1991; Sratton 1999; Williamson *et al.* 1995). Moreover, for some variables and processes in some regions, the simulation degrades as the resolution becomes higher (Boyle, 1993). There have been a number of studies concerned with the assessment of the effects of varying horizontal resolution on GCM simulations - for example: Stratton (1999) using the Hadley Centre climate model; Hasegawa *et al.* (1997) and Williamson *et al.* (1995) using NCAR CCM2 GCM; Boyle (1993) and Phillips *et al.* (1995) using the ECMWF; Boville (1991) using NCAR CCM1 GCM and Lal *et al.* (1997) using ECHAM3 GCM. All studies of resolution tend to confirm that the finer scales are required to capture the non-linear processes that force the medium scales, concluding that, at a minimum, 2.5° resolution is required to represent the general circulation adequately. Increasing resolution tends to increase the high frequency variability of the model and so the eddy kinetic energy, though this does not always represent an improvement of the simulation.

In this study the Hadley Centre Atmospheric Model version 2b (HadAM2b) is analysed focusing on the SH circulation. An extensive evaluation of the HadAm2b climate model was made by Stratton (1999), who examined the standard and high resolution integrations performed with the model using the AMIP-style forcing for the period 1979-1988. Concerning the dynamical aspects, the results of her work can be summarised as follows: most of the systematic errors in the AMIP simulations appear to be almost independent of resolution, though greater detail, as might be expected, comes from the ability of the higher resolution model to resolve smaller scale features. This results in a poleward shift in the westerly jets and enhanced high frequency variability (through increased eddy kinetic energy, momentum fluxes and heat fluxes in the latitudes of the storm tracks). The evaluation of the standard and high-resolution integrations in Stratton (1999) has been made on a global basis. Due to the unique characteristics of the circulation patterns of the SH mentioned above, in this work we focus on the evaluation of regional features in the SH with special emphasis on the South American region.

The aims of this paper are twofold: to evaluate the ability of the HadAm2b GCM to simulate the transient behaviour of the atmospheric circulation in the SH and to assess the impact of increasing resolution on these transient features.

Model fields are compared with observational climatologies, described in Section 2, to assess the model simulation at both resolutions. A complete description of the model is given in Stratton (1999) and will not be repeated here.

Some relevant features of the mean climate simulated at the standard and high resolutions are compared with climatology (Section 3). A comparison of some transient diagnostics is given in Section 4, and a summary of the strengths and deficiencies of the simulations and results is presented in Section 5.

2. Data sets

The standard (2.5° latitude by 3.75° longitude) and high-resolution (0.833° latitude by 1.25° longitude) AMIP integrations performed with the HadAM2b atmospheric GCM are compared with analyses of observed data.

The data base used in this study consists of 10 years (1979-1988) of daily 0000 UTC geopotential height, winds and temperature at six vertical levels (850, 700, 500, 300, 200 and 50) and sea level pressure, produced by the HadAM2b high resolution model. Standard resolution output is available only for four vertical levels (850, 500, 200 and 50).

Both model AMIP runs started from the beginning of December 1978 and continued for 10 years and one month. The first month of each run was treated as a spinup and was not included in the analysis.

The analyses used to evaluate the models consist of 10 years (1979-1988) of National Center for Environmental Prediction (NCEP) daily 0000 UTC re-analysis data set (Kalnay *et al.,* 1996) and, for seasonal eddy properties only, the European Centre for Medium-Range Weather Forecasting

re-analysis (ERA) data set, for the same time sampling. They represent the most complete, physically consistent atmospheric data sets and have been used for a wide range of studies in the SH. Though, as known, the NCEP re-analysis data set has been contaminated by misplacement of PAOBS (SH surface pressure bogus data produced by Australia) for the years 1979-1992, discussions about its quality on a monthly mean and daily basis over the SH (Garreaud and Battisti, 1999; Simmonds and Keay, 2000; Renwick and Revell, 1999; Kistler *et al.,* 2001; Solman and Menéndez, 2002), have largely demonstrated they are suitable for studies in the SH on daily timescales.

As shown in Li and Carril (1998) some systematic differences between NCEP re-analyses and ERA can be found over poor-data regions of the Southern Hemisphere. More specifically, both the zonal mean wind and the transient variability, are weaker in NCEP re-analysis data set than in ERA, probably due to the differing spatial resolutions of the data assimilation systems and model physics differences. Overall, the mean fields are in good agreement and so are only shown for NCEP. We consider that it is important to keep in mind this aspect of the data sets used to validate the models particularly since, as will be shown, HadAm2b at both resolutions seems to systematically overestimate eddy quantities, relative to the NCEP data and generally compare better with ERA.

Transients are defined here by removing the seasonal cycle and the seasonal mean for each winter season, which filters out the interannual variability from the time series. No further filtering of the time series was performed. Winter season is defined here as the period from 1 June to 31 August and summer season is defined as the period from 1 December to 28 February.

After calculations of several diagnostic fields were done, both model results were interpolated to the NCEP grid (2.5° latitude by 2.5° longitude) for comparison purposes.

3. Mean climate

3.1 Mean sea level pressure

The mean sea level pressure (SLP) pattern is a useful measure of an atmospheric GCM's ability to simulate the atmospheric circulation near the surface and it represents an integrated measure of the model´s thermodynamic and dynamic performance. It also portrays the background flow against which synoptic disturbances develop, which is one of the interests of this paper.

Figures 1a and 1b show the averaged SLP patterns for DJF and JJA, respectively, for the Southern Hemisphere (SH). Both models represent the basic observed patterns quite well, though some differences can be remarked. In both seasons the subtropical belt of high pressure is slightly shifted poleward and overestimated in both runs. The circumpolar Antarctic trough is well positioned though central pressures are deeper than observed, resulting in stronger westerlies and shifted poleward, compared with observed climatology. Differences on the strength of the circumpolar trough are larger during southern winter (JJA) and, as a consequence, the westerly bias is larger.

The differences pointed out are generally more dramatic for the high resolution run, indicating that increasing resolution increases systematic errors in SLP. For an objective verification of the SLP field see Table 3 of Stratton (1999).

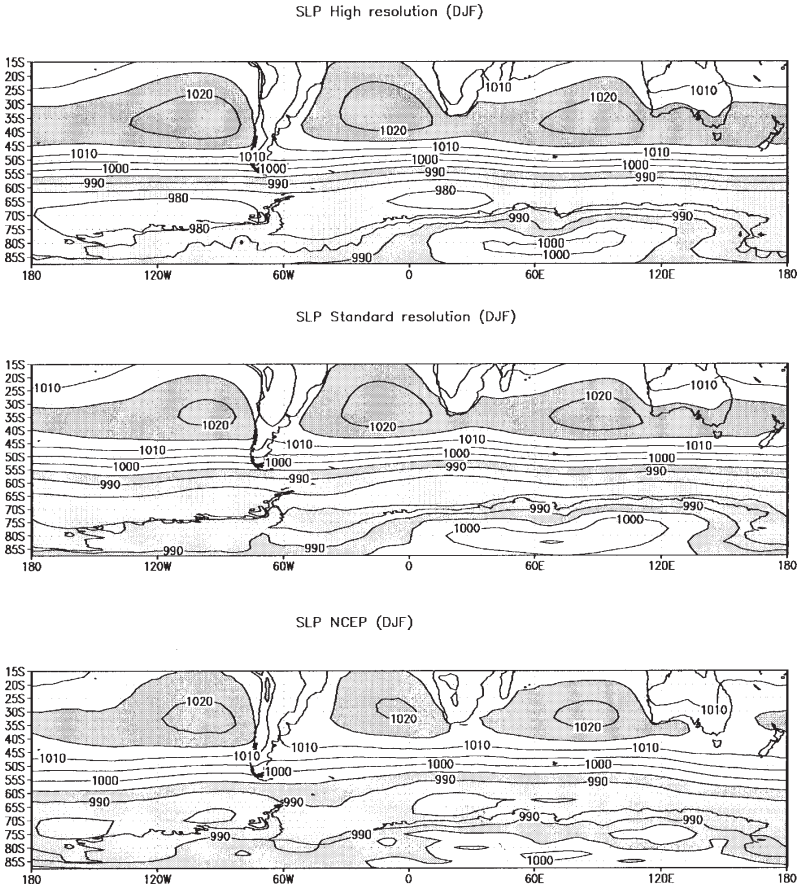

Fig. 1a. Mean DJF sea level pressure from High resolution (top), Standard resolution (centre) and NCEP climatology (bottom). Contours every 5 hPa with values higher than 1015 hPa and lower than 995 hPa shaded.

3.2 Upper level zonal wind

The horizontal wind distribution is closely linked geostrophically to the temperature and pressure distributions. The zonal wind, in particular, has traditionally been one of the fundamental climate simulation verification parameters. Figures 2a and 2b show the zonal wind structure at 200 hPa for DJF and JJA, respectively.

For DJF both models reproduce the zonal asymmetries of the zonal wind quite well, with a maximum in the eastern Atlantic - western Indian Ocean. At both resolutions the westerly jet is too zonally elongated, too strong and shifted poleward, in agreement with the SLP field discussed

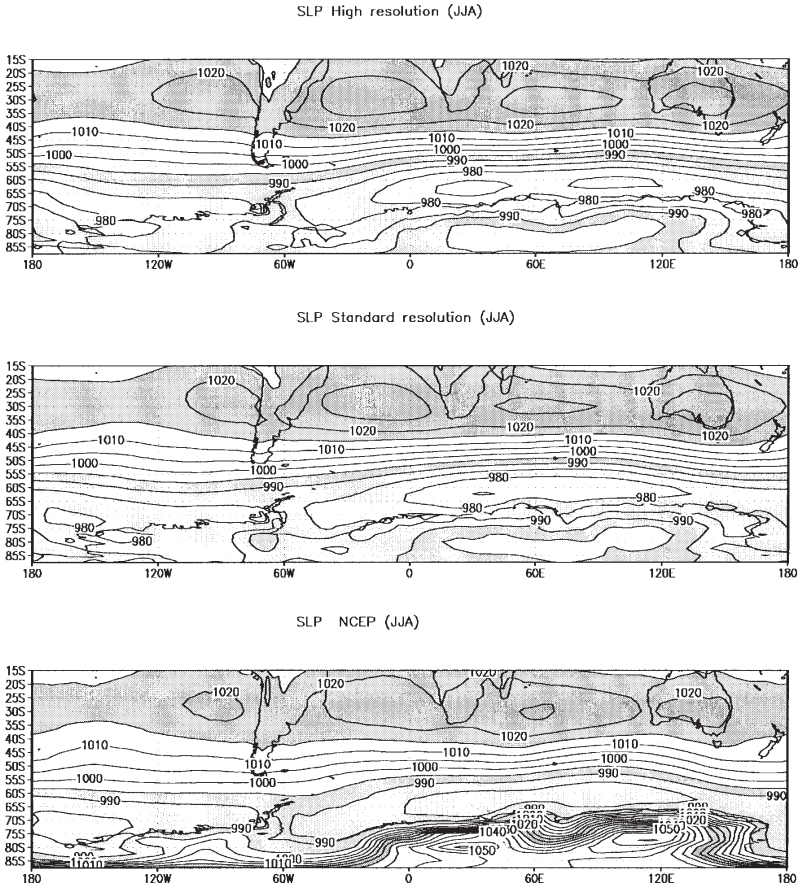

Fig. 1b. As in Fig. 1a but for JJA.

before. The strongest westerlies extend too far east south of Australia, where both models overestimate the upper level westerlies by more than 10 m/s. The easterly bias between 15° S and 30°S present in both model runs, is increased at high resolution due to the poleward shift of the westerly jet. In general, the deficiencies observed are again stronger at high resolution.

During the winter season a well-defined split jet structure can be seen in the analyses over eastern Australia with a polar branch extending over the Pacific Ocean around 60° S and a sub-tropical branch centred at 30° S. This wintertime split jet structure is also apparent in the simulations at both resolutions, but the polar branch of the westerlies is located further north than in the analyses and does not extend far enough east over the Southern Pacific. The subtropical jet simulated at both resolutions is stronger and shifted poleward, compared with observations. The models do not capture the maximum over Australia and both simulations only exhibit the maximum located further

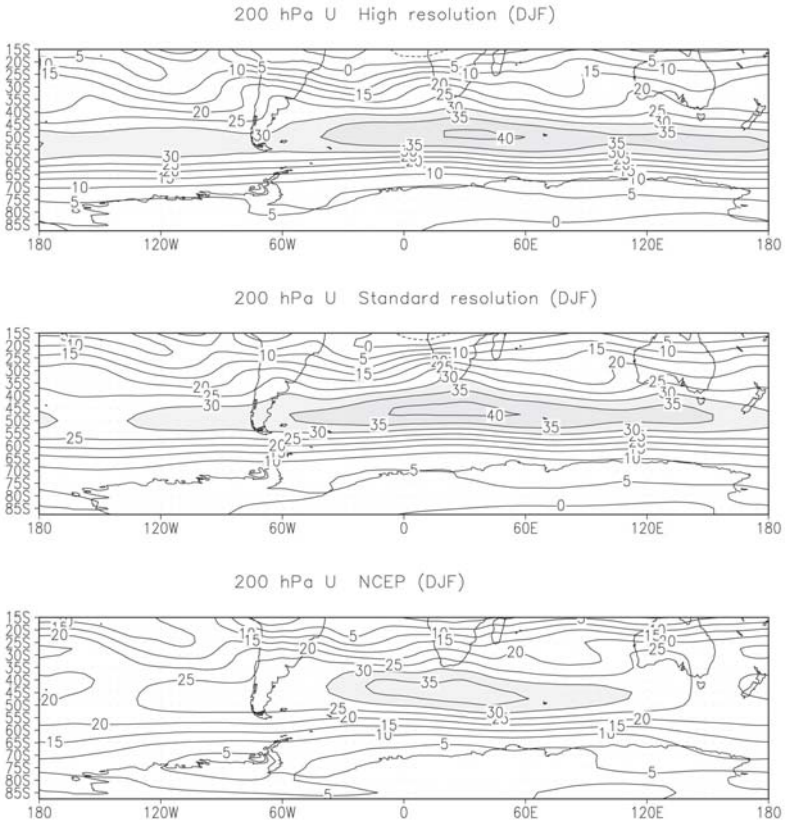

Fig. 2a. Mean DJF zonal wind at 200 hPa from High resolution (top), Standard resolution (centre) and NCEP climatology (bottom). Contours every 5 m s^{-1} with values larger than 30 m s^{-1} shaded.

eastward. The changes in the zonal wind field due to increasing resolution do not represent an improvement in the simulated climate.

These errors in the jet representation are common in other GCMs and are almost independent of resolution. For example, Katzfey and McInnes (1996) with the CSIRO GCM (R21 resolution) and Hurrell *et al.* (1998) with the CCM3 GCM (T42 resolution) have found similar deficiencies in the jet structure. Even in high-resolution simulations (Boville, 1991; Williamson *et al.,* 1995) the horizontal wind does not clearly exhibit the observed split jet stream feature.

The temperature fields are not shown, as the results are analysed in detail in Stratton (1999) and agree with other authors. The main results are that the high-resolution model tends to reduce the

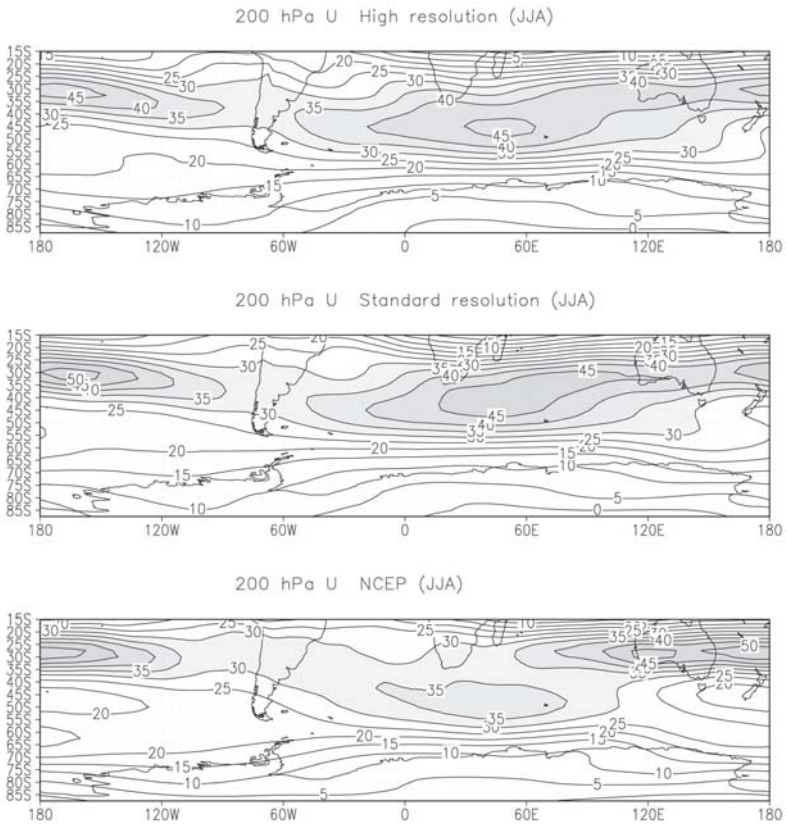

Fig. 2b. As in Fig. 2a but for JJA.

cold bias in the troposphere, with larger increases occurring in mid-latitudes, in the regions where the westerly jets have shifted poleward. In these regions, the lower troposphere, below 500 hPa, is even warmer than in the analyses, especially in the summer months. The warming of the troposphere at high resolution is explained by the more intense vertical motion leading to a more active hydrological cycle and a greater release of heat due to condensation and also by more intense poleward heat flux, which is maximum at lower levels, due to more active eddies, as will be shown later in this paper.

3.3 Mean baroclinicity

A useful local measure of the susceptibility of the basic state to baroclinic instability is the growth rate of the fastest growing Eady wave (Lindzen and Farrel, 1980; Hoskins and Valdes, 1990).

This quantity is defined by:

$$\sigma_{BI} = \frac{0.31 f}{N} \left| \frac{\partial U}{\partial z} \right|$$

where f is the Coriolis parameter, N is the Brunt-Vaisala frequency, U is the horizontal wind vector and z the vertical coordinate.

¿? The **Eady** growth rate computed at lower levels of the atmosphere (850 – 500 hPa layer) is plotted in Figures 3a and 3b for DJF and JJA, respectively.

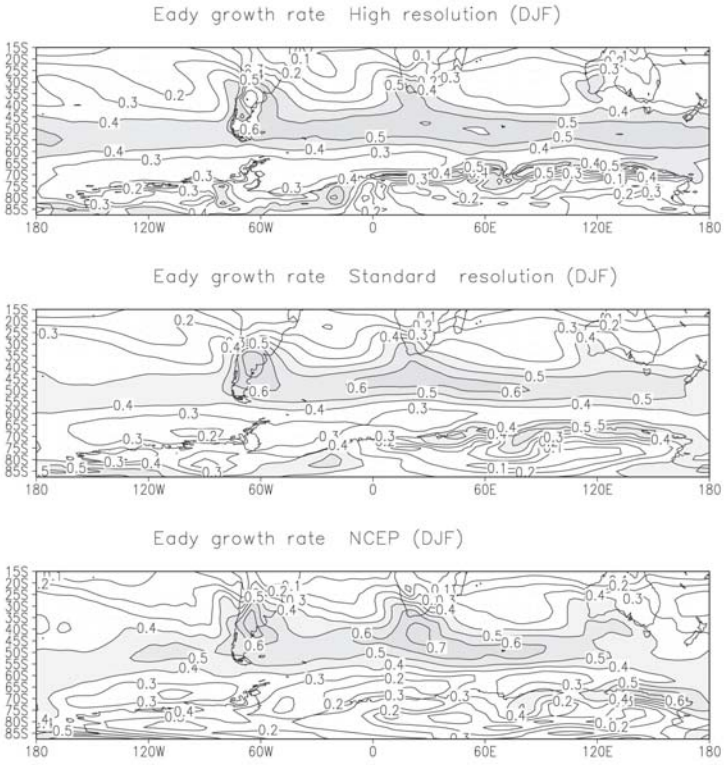

¿? Fig. 3a. **Eady** growth rate for DJF computed for the 850-500 hPa layer from High resolution (top), Standard resolution (center) and NCEP climatology (bottom). Contours every 0.1 day $^{-1}$ with values larger than 0.4 day $^{-1}$ shaded.

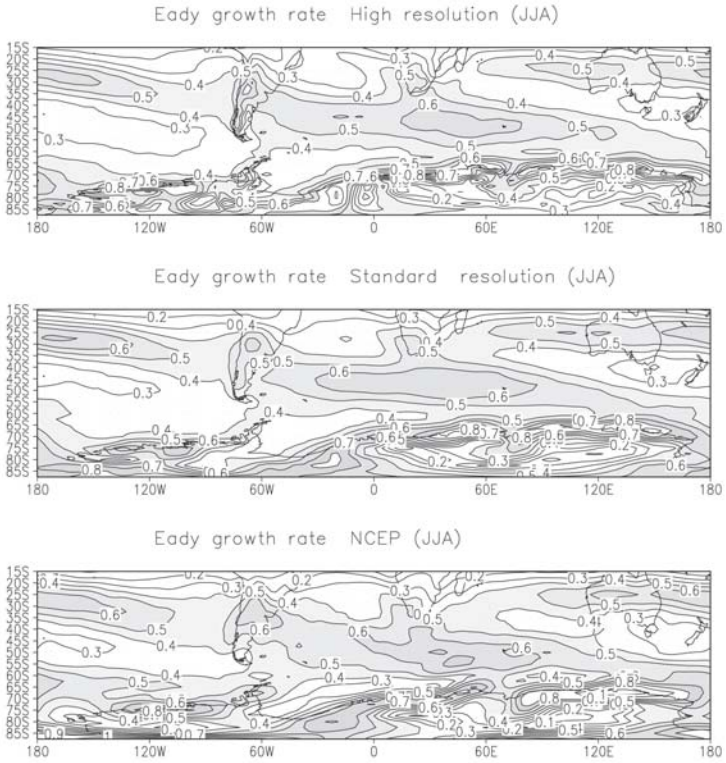

Fig. 3b. As in Fig. 3a but for JJA.

For summer months (DJF) the regions of maximum Eady growth rate are reasonably well simulated by both models, though shifted poleward compared with the analyses, in agreement with the structure of the westerlies. A striking feature of this quantity is that in the high resolution run the maxima of eddy growth rate in the eastern Pacific Ocean and the eastern Atlantic - western Indian Ocean are smaller than at standard resolution and are also smaller than the analyses. In agreement with the results of Hoskins and Valdes (1990) for the NH and Berbery and Vera (1996) for the SH, the pattern of eddy growth rate is largely modulated by the shear term, while the static stability term is almost constant everywhere (not shown). Nevertheless, the static stability at lower levels simulated with the high-resolution model is larger than the analyses, due to the middle troposphere warming. Moreover, the high resolution run overestimates even more the vertical stability of the atmosphere at lower levels than the standard resolution run. On the other hand, the model at both resolutions underestimates the vertical shear of the horizontal wind at lower levels, and, in consequence, this measure of baroclinicity is weaker than observed.

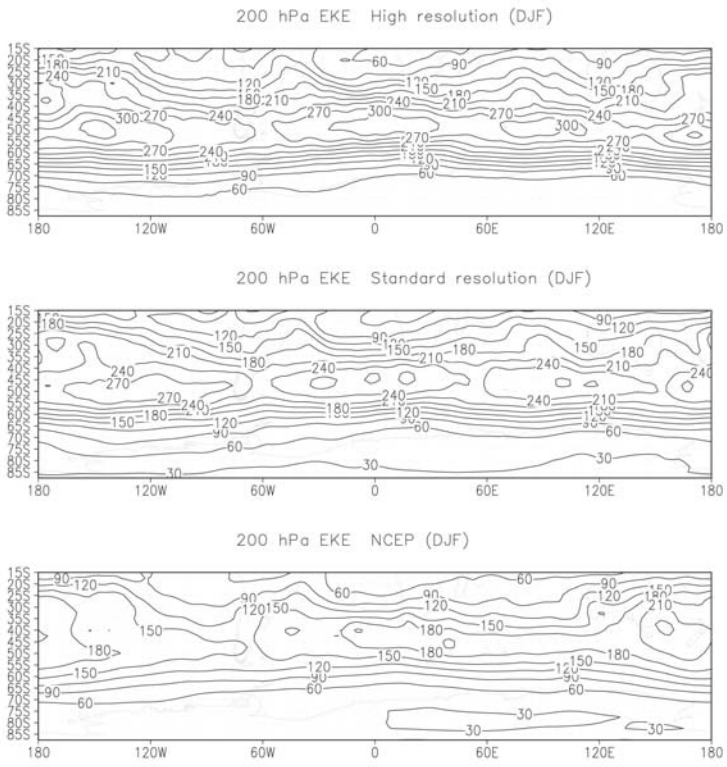

Fig. 4a. Mean DJF eddy kinetic energy at 200 hPa from High resolution, Standard resolution, NCEP climatology and ERA climatology. Contours every 30 $m^2 s^{-2}$.

For the winter season the split jet feature is reflected in regions of maximum σ_{BI} for both resolutions, though somewhat underestimated in the exit region of the polar storm track over the South-eastern Pacific Ocean at both resolutions. The Atlantic and Indian Ocean storm tracks, represented by regions of relatively large values of $\sigma_{BI,}$ are shifted poleward compared with the analyses for both model resolutions, this displacement being larger for the high resolution run, in agreement with the poleward shift in the westerlies. Nevertheless, the areas of maximum σ_{BI} over the Atlantic-Indian Oceans and over Australia are better simulated by the high-resolution model.

4. Transient eddy diagnostics

The transient behaviour of the atmospheric circulation is an important component of the general circulation. The meridional fluxes of eddy quantities such as heat and momentum play a key role in determining the mean circulation in the atmosphere, as they are responsible for reducing the

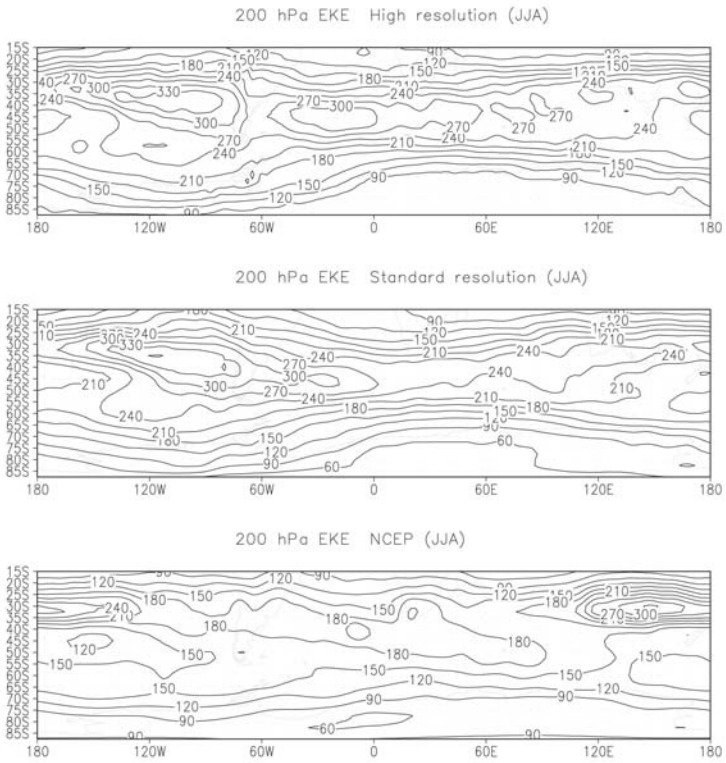

Fig. 4b. As in Fig. 4a but for JJA.

temperature gradients and horizontal wind shears in midlatitudes and in transporting heat and momentum out of the subtropics and into higher latitudes. These transient meridional transports are much stronger than the stationary meridional transport in SH (Peixoto and Oort 1984).

In this section we concentrate on various measures of transient activity in order to assess the ability of the model in reproducing some characteristic features of storm-track activity in the SH.

The transient activity of the models is assessed by analysing the transient eddy kinetic energy, displayed in Figure 4, the transient eddy momentum flux at 200 hPa (both quantities peak at upper levels of the troposphere) and the transient heat flux at 850 hPa, which peaks in the lower troposphere (summarised on Table 1). The horizontal structure and temporal evolution of synoptic-scale waves during SH winter has also been analysed and are described in Figures 5 and 6.

Table 1. Zonal mean eddy momentum flux at 200 hPa (in $m^2 s^{-2}$) and eddy heat flux at 850 hPa (in km s^{-1}) averaged over for 10° latitude belts, centred at 20° S, 30° S, 40° S, 50° S, 60° S and 70° S, respectively.

		DJF			JJA		
		High res.	Std res.	NCEP	High res.	Std res.	NCEP
Eddy	15S-25S	-12.8	-13.5	-12.8	-28.6	- 8.4	-21.8
momentum	25S-35S	-40.5	-35.8	-38.1	-72.5	-52.7	-56.8
flux	35S-45S	-65.2	-48.8	-44.4	-72.6	-70.9	-42.1
	45S-55S	-39.7	-25.3	-16.8	-23.8	-32.0	-14.8
	55S-65S	4.3	4.1	5.1	20.12	7.7	15.3
Eddy	15S-25S	- 1.5	- 1.6	- 1.1	- 4.2	- 2.8	- 2.9
heat flux	25S-35S	- 6.6	- 5.1	- 6.4	- 9.8	- 7.3	- 8.4
	35S-45S	-11.2	-11.5	-11.0	-17.2	-18.1	-14.6
	45S-55S	-14.7	-14.8	-12.9	-22.6	-23.7	-18.1
	55S-65S	-10.5	- 7.4	- 6.6	-25.0	-21.1	-15.2
	65S-75S	- 3.8	- 2.9	- 5.5	-18.1	- 9.1	-10.5

4.1 Eddy kinetic energy

The eddy kinetic energy is an overall measure of the amplitude of baroclinic disturbances and is used to characterise the storm-tracks. The eddy kinetic energy, defined as $(u'^2 + v'^2)/2$, where u' and v' denote transients, is depicted in Figures 4a and 4b, for DJF and JJA, respectively. Before analysing these eddy quantities it should be taken into account that, as was shown in Stratton (1999), the maximum in eddy kinetic energy and eddy momentum flux occur higher in the atmosphere for both model simulations compared with ERA climatology, particularly for the high resolution model; this is connected with the model tropopause being higher than observed (Stratton, 1999). We have to be careful also when comparing the magnitude of eddy quantities against NCEP re-analyses in the SH. Large discrepancies between ERA and NCEP re-analysis have been pointed out in an article by Li and Carril (1998), particularly over data-poor regions, where the transients properties in NCEP are systematically weaker (about 20%) than those in ERA. Observed transient fields from both NCEP and ERA climatology are depicted in the following figures, though any comparison between both re-analysis data sets is beyond the scope of this article.

A primary difference from observations is that the high frequency variability, in terms of the eddy kinetic energy, for both summer and winter seasons, is overestimated by HadAm2b when compared against NCEP climatology, at both resolutions, though its location is generally good. The model eddy intensities are realistic when compared against ERA, though the high-resolution model overestimates the peaks and shifts them poleward. Thus, we are going to concentrate mainly in the spatial distribution of these quantities rather than the magnitude.

In agreement with both climatologies, the simulated maximum eddy kinetic energy over the SH encircles the globe between 40° and 55° S during summer, but during winter it shifts equatorward over the Pacific and the Atlantic Oceans and spirals poleward over the Indian Ocean toward the

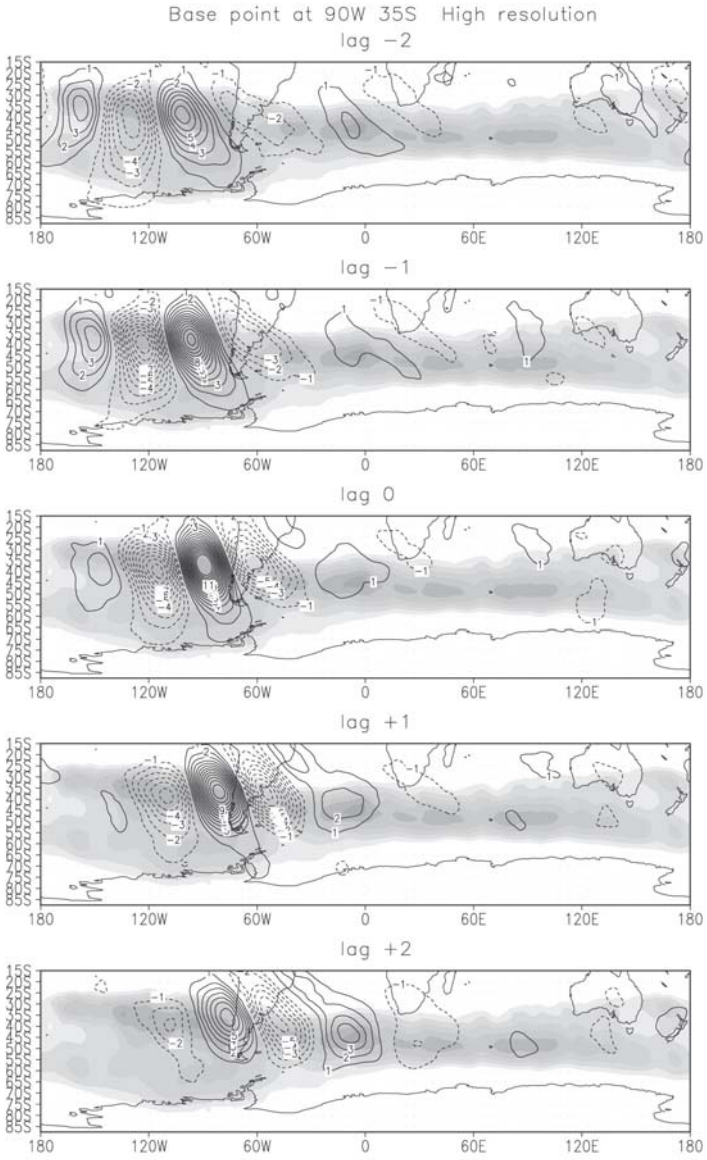

Fig. 5a. Regression for the meridional component of the wind at 200 hPa with a base point at 35° S, 90° W from lag (day) -2 to 2 for High resolution. Contours every 1 m s^{-1}, zero contour is omitted. The shaded area represents the variance of meridional wind at 200 hPa larger than 180 $m^2 s^{-2}$.

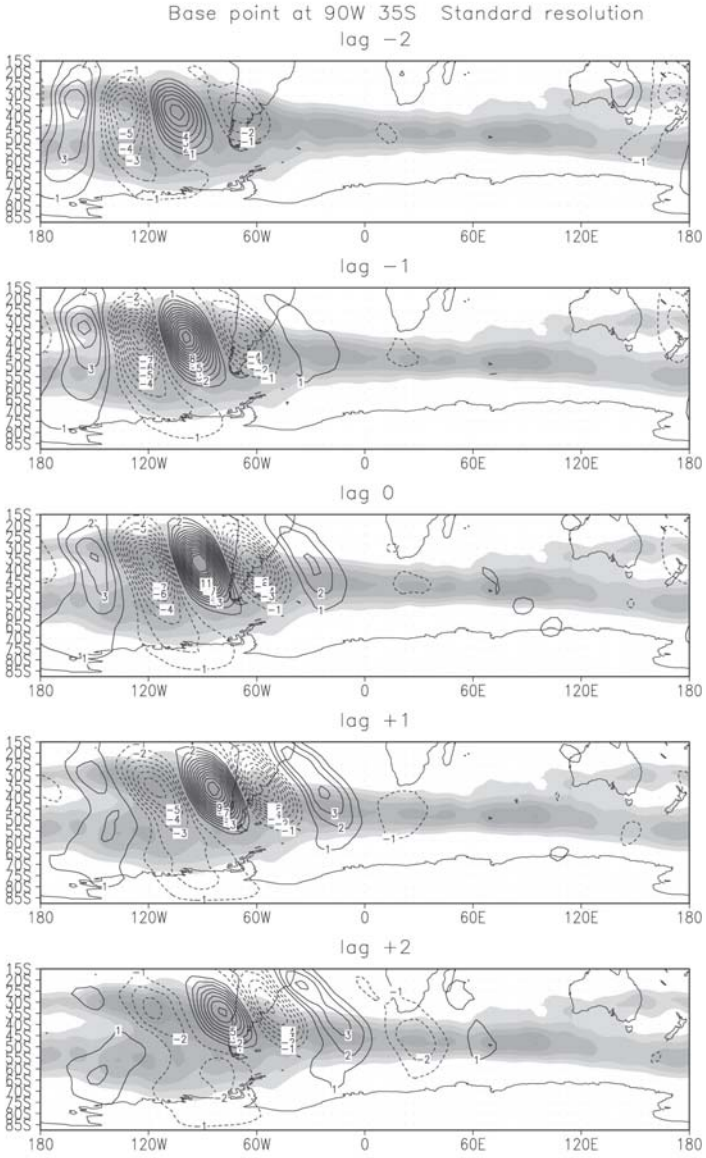

Fig. 5b. As in Fig. 5a but for Standard resolution.

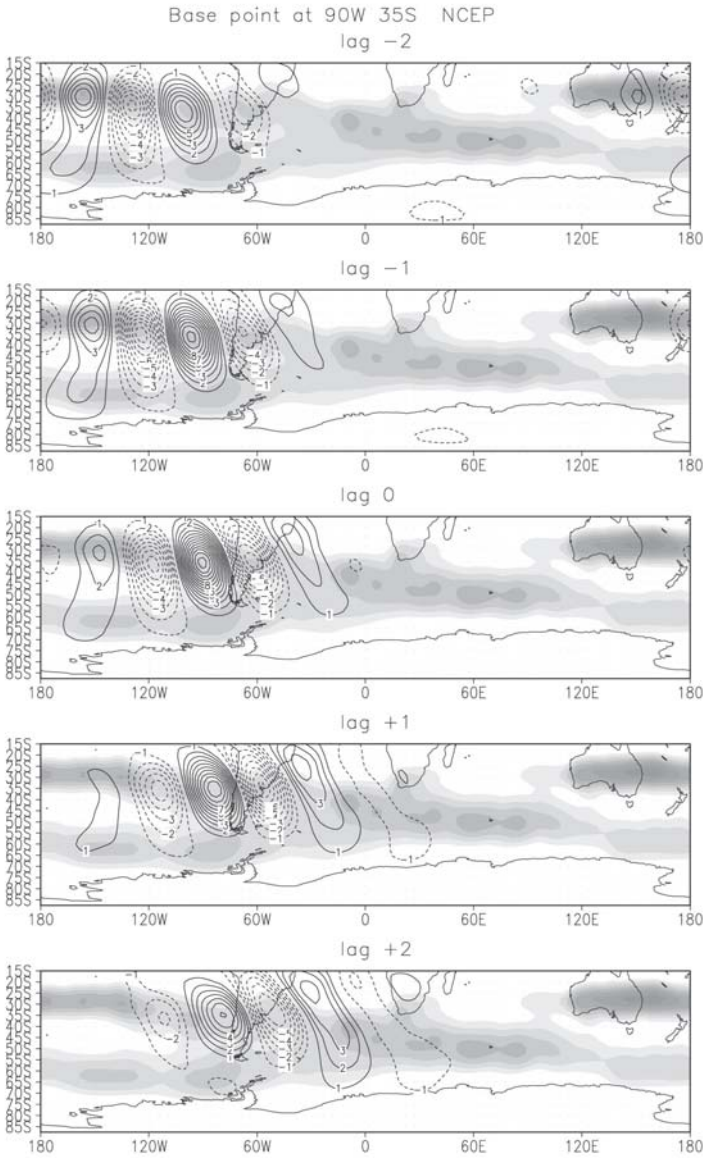

Fig. 5c. As in Fig. 5a but for NCEP climatology.

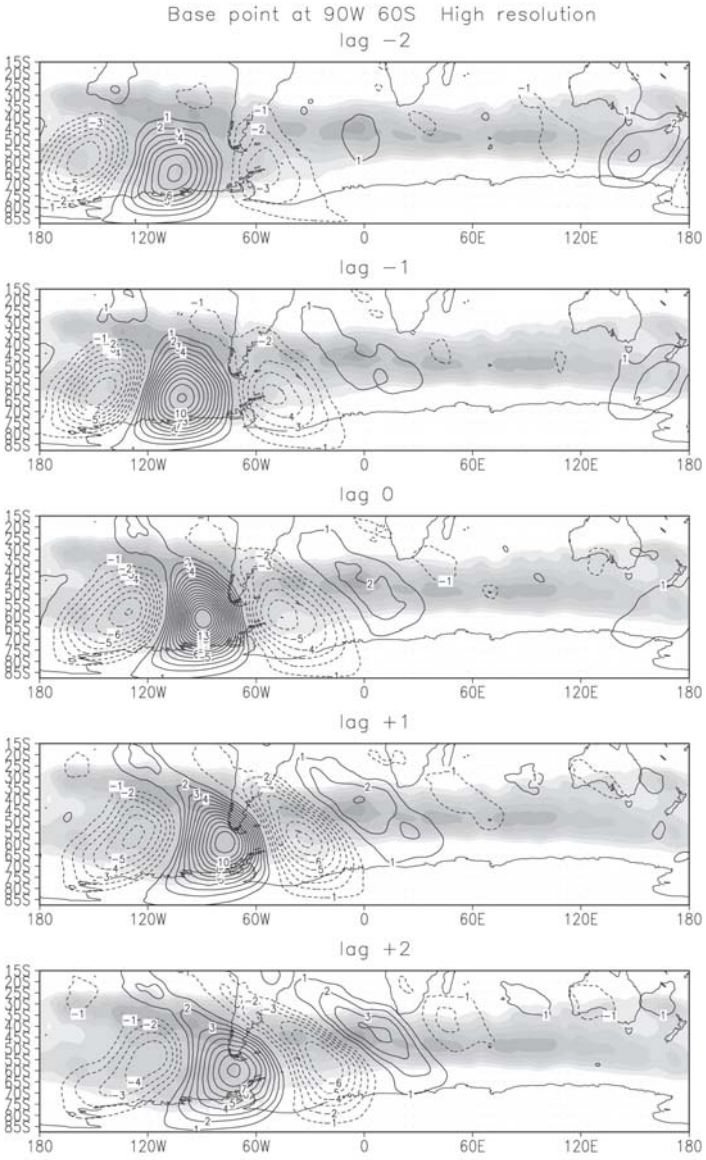

Fig. 6a. Regression for the meridional component of the wind at 200 hPa with a base point at 60° S, 90° W from lag -2 to 2 for High resolution. Contours every 1 m s^{-1}, zero contour is omitted. The shaded area represents the variance of meridional wind at 200 hPa larger than 180 $m^2 s^{-2}$.

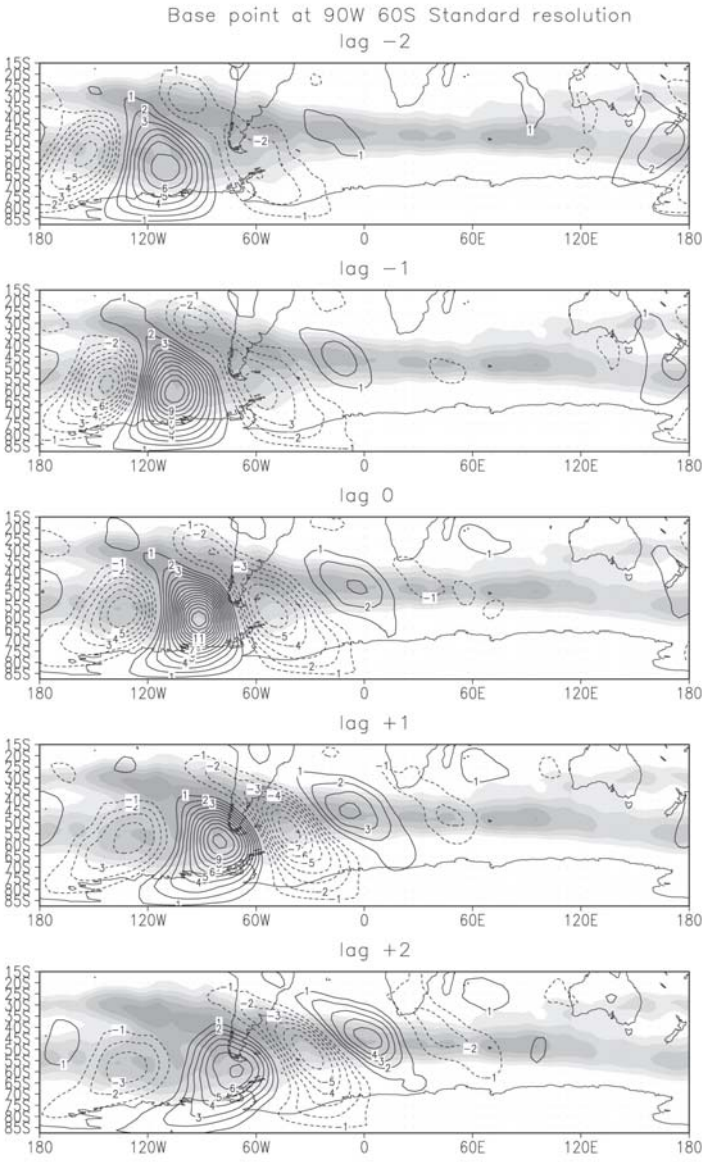

Fig. 6b. As in Fig. 6a but for Standard resolution.

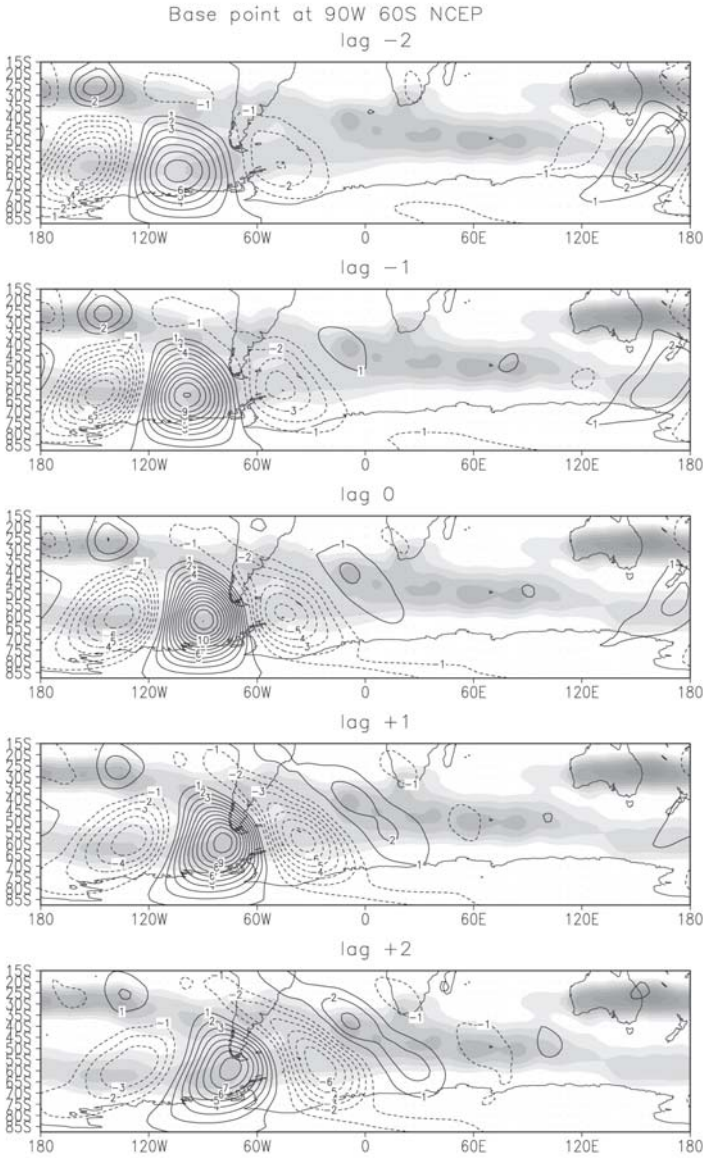

Fig. 6c. As in Fig. 6a but for NCEP climatology.

Pacific. The result is a double maximum with minimum values over New Zealand, a feature also evident in the observed and simulated 200 hPa zonal winds. The areas of maximum eddy kinetic energy expand latitudinally during winter, reflecting the enhanced daily variability of the polar and subtropical jetstreams. This feature is well captured by both models.

In both seasons the regions of maximum variability, in terms of EKE, are well captured by both models, though some discrepancies can be found concerning the zonal asymmetries. The largest differences occur over Australia during winter season, where HadAM2b is not capable of simulating the observed maximum. Instead, both models simulate a maximum further eastward in the eastern Pacific Ocean.

It is important to remark that the magnitude EKE increases with resolution and, during both summer and winter months, there is a poleward shift with increasing resolution, as was evident in the mean wind field. For winter season, the poleward shift in EKE is observed over the Atlantic storm-track and the subtropical branch of the Pacific storm-track. On the contrary, the polar branch of the Pacific storm-track close to the dateline is shifted equatorward (centred between 55° and 60° S for the high resolution model, 55°S for the standard resolution model and between 60° and 65°S for the analysis).

4.2 Meridional momentum and heat fluxes

The upper level eddy momentum fluxes and eddy heat fluxes are summarised in Table 1, which shows the zonal mean values for different latitudinal belts for DJF and JJA, respectively. The transient momentum flux tends to be stronger and shifted poleward for the high-resolution model, and the enhanced momentum flux convergence is consistent with westerly wind biases evident at 200 hPa. Another important feature is the latitudinal extension of the maxima, which is better simulated with the high-resolution model for both summer and winter seasons. Increasing the resolution results in increasing the transient momentum flux and in shifting the areas of maximum flux poleward.

In the lower troposphere HadAM2b at both resolutions the model successfully simulates the major features of the meridional heat flux. The regional features of eddy heat flux are captured for both models, the location being better simulated with the high-resolution model (not shown). In Table 1 it can be seen that the high-resolution model tends to shift the regions of larger poleward heat flux to higher latitudes, in agreement with the fact that the disturbances are more intense and, in consequence, they are more efficient in redistributing the heat towards the pole. This is more marked during winter season (JJA), when the high-frequency activity is larger.

4.3 Structure and evolution of synoptic-scale disturbances

Figure 4 provides a general view of the regions where maximum variability occurs. In order to assess the realism of the synoptic-scale wave structure in the models, one-point contemporaneous and time-lag regressions of the meridional component of the wind at 200 hPa were computed. This

technique has been used by several authors to determine the structure and evolution of the transient disturbances. Lim and Wallace (1991) performed a regression analysis of various fields to the 500 hPa heights to describe many features of waves and wave packets in the northern Pacific Ocean. In their analysis they found a structure that was suggestive of an evolving 'generic' baroclinic wave. In a similar type of analysis, Berbery and Vera (1996) used correlation analysis of the meridional component of the wind to investigate the characteristics of the Southern Hemisphere winter storm track. They found that the unfiltered meridional wind component was adequate to represent the features of synoptic-scale eddies and that wave packets show a decay of upstream centres as new ones grow downstream, suggesting that downstream development contributes to the evolution of the synoptic-scale waves in the SH winter storm track. This process is observed both in the subpolar and subtropical jets, but the sequence of centres developing downstream is more coherent in the latter. Solman and Menéndez (2002), used this technique to characterize the interannual variability associated to ENSO of winter storm tracks over the south Pacific- South Atlantic sector.

In this study we focus on the structure of waves that develop during austral winter months in the South American sector and, hence, we concentrate on those synoptic systems that interact with the Andes mountains, which is one of the most important topographic features in the region. Lagged regressions of the 200 hPa meridional wind component were computed, similarly to Lim and Wallace (1991), to analyse the evolution of waves that develop within the subtropical and subpolar branches of the eastern Pacific storm-track, thus giving emphasis to upper level perturbations. We selected base points at 35°S, 90°W and 60°S, 90°W, i.e., at the exit region of the subtropical and subpolar branches of the Pacific storm track, respectively.

Figure 5 displays the temporal evolution of the waves that develop within the subtropical branch of the Pacific storm-track (choosing a base point at 35°S, 90°W) for the high resolution model (a), the standard resolution model (b) and NCEP re-analysis (c), respectively. Superimposed to the regression coefficients, the variance of the meridional component of the wind at 200 hPa, a measure of the high frequency variability, is also shown.

The regression coefficients for the analysis (Figure 5c) show that fluctuations at upper levels follow a mainly zonal path west of the Andes, while further east they acquire a northeastward direction. Gan and Rao (1994) attribute such behaviour in the high frequencies to an orographic effect of the Andes mountains, in agreement with similar equatorward direction discussed by Wallace et al. (1988) for the waves east of the Rockies. The structure is that of a wave with a wavelength of the order of 5200 km, which reduces over the continent to 5000 km and a longitudinal extension of the wave packet of the order of 2.5 wavelengths, in agreement with Berbery and Vera (1996). The temporal evolution of the wave packet reveals that upstream centres decay as new ones grow downstream maintaining the total extent of the wave packet constant during the whole sequence. Changes in the orientation of the wave centres observed during the wave packet evolution show that in the early stages the wave centres have a north-south axis but as the wave approach the Andes they become more meridionally elongated and they acquire a NW-SE orientation. These

larger meridional tilts are related to larger momentum flux (see Table 1). Lim and Wallace (1991) and Chang (1993) observed a similar structure of patterns in the Northern Hemisphere over the Pacific Ocean.

The structure of the waves in the high resolution and standard resolution simulations (Figures 5a and 5b, respectively) are very similar to those in the analysis, for the wavelength, the extension of the wave packet and the temporal evolution, indicating that the simulated wave structure in the models is realistic, though the regression coefficients are larger than in NCEP data. This means larger amplitude of the waves, in agreement with larger values of eddy kinetic energy discussed before. Both models capture the north-eastward propagation of the waves in the vicinity of the Andes, though the NW-SE tilt on the lee side is slightly overestimated, in agreement with the larger eddy momentum flux. In both simulations the characteristic length of the wave packet over the Atlantic Ocean is larger than in NCEP. It is also noticeable that the meridional extension of the Atlantic Ocean storm - track is more confined in both simulations compared with NCEP and the waves tend to be more meridionally confined as well.

Comparing Figures 5a, 5b and 5c it can be concluded that the patterns obtained for the high resolution simulation do not represent any significant improvement in the simulation of the high frequency disturbances that develop within the subtropical branch of the Pacific storm-track compared with the standard resolution simulation. Both models reproduce the structure of the waves reasonably well.

The evolution of the waves that develop within the polar branch of the Pacific Ocean storm-track is depicted on Figure 6 (base point at 60°S, 90 °W). The regression coefficients for the analysis show that the waves have a characteristic wavelength of 5600 km and the extension of the wave packet is about two wavelengths. The orographic effect of the Andes, concerning the change in the tilt of the waves and the north-eastward propagation as they approach the continent is more marked than for the waves that propagate within the subtropical branch of the storm-track, in agreement with Gan and Rao (1994).

HadAm2b is capable of simulating the evolution of these waves, though the characteristic wavelength is smaller and the amplitude of the waves is larger for both the high resolution and the standard resolution simulations. In agreement with the northward shift of the polar branch of the Pacific storm-track, the waves that develop over the Pacific Ocean tend to be shifted equatorward as well for both model resolutions. This is associated with the structure of the polar branch of the westerlies, which is located further north than in the analyses. The orographic influence of the Andes mountains, concerning the northeastward propagation of the waves as they approach the continent is better resolved in the high-resolution simulation. The high-resolution simulation better represents the overall evolution of the wave packet.

5. Summary and conclusions

In this paper we have evaluated the capability of the HadAm2b version of the Hadley Centre atmospheric general circulation model to simulate the circulation patterns on the Southern

Hemisphere, with particular emphasis on the high frequencies. The impact of changing resolution has also been addressed by comparing a high-resolution (0.833° latitude by 1.25° longitude) AMIP simulation with a standard resolution experiment (2.5° by 3.75°) and observed climatology (at 2.5 ° by 2.5°).

At sea level both models reproduce the basic observed patterns of the pressure field quite well, though some discrepancies can be found. As in other studies focused on the impact of resolution, in both seasons the subtropical belt of high pressure is slightly shifted poleward and overestimated in both runs. The circumpolar Antarctic trough is well positioned though central pressures are deeper than observed, resulting in westerlies which are stronger and shifted poleward, compared with observed climatology. Differences in the strength of the circumpolar trough are larger during southern winter and, as a consequence, the westerly bias is larger. The differences pointed out are generally more dramatic for the high resolution run, suggesting that increasing resolution does not seem to reduce systematic errors in SLP.

The simulation of the upper level flow in both seasons, concerning the zonal asymmetries, is very good for both model resolutions, though the westerly jet is too zonally elongated, too strong and shifted poleward, consistent with the SLP field. The deficiencies observed are larger at high resolution. Both models successfully reproduce the split jet structure of the Southern Hemisphere winter, with the polar branch of the westerlies over the Pacific Ocean being further north than in the analysis. Overall, the changes in the zonal wind field due to increasing resolution do not represent an improvement in the simulated climate.

In order to evaluate the performance of the model in capturing the characteristics of transient quantities and, taking into account the mentioned differences between NCEP re-analyses and ERA concerning the intensity of eddy quantities, we have included eddy fields from ERA climatology for comparison. Overall, the model eddy intensities are realistic when compared with ERA, but overestimated when compared with NCEP. Nevertheless, the basic shapes of the eddy fields from the model at both resolutions compare reasonably well with both climatologies. The upper level storm-tracks, in terms of the eddy kinetic energy, are reasonably well simulated, and though overestimated at both resolutions compared with NCEP, have generally similar intensities to those in ERA analyses. The magnitudes of the eddy kinetic energy, momentum fluxes and heat fluxes in the latitudes of the storm tracks increase with resolution. This might be expected, as the higher resolution model should be able to resolve smaller scales, implying that individually storms may be more intense. This agrees with other published studies of resolution (Boville, 1991; Stratton, 1999). For winter months the storm-track over the Atlantic and Indian Oceans is shifted poleward compared with the analysis and the polar branch of the Pacific storm-track is located further north than in the analysis. The locations of the areas of maximum eddy kinetic energy are shifted southward with increasing resolution. Although increasing resolution does not improve the general features of the high frequency variability, some regional features, such as the Pacific storm-track during summer with maximum activity near the date-line, the subtropical branch of the Pacific storm-track and the Atlantic storm-track during winter, are better simulated with the high-resolution model.

The structure and evolution of the synoptic-scale waves in the winter storm-track of the Southern Hemisphere were analysed for both model resolutions and compared with NCEP re-analysis data. Time-lag regression analysis for the meridional component of the upper level wind at two selected base points (located at the exit region of the subtropical and polar branches of the Pacific storm-track, respectively) were computed in order to determine the 'mean' baroclinic wave structure and its temporal evolution of the simulations.

For waves developing within both the subtropical and polar branches of the Pacific storm-track, both models captured the baroclinic wave structure very well, in respect of wavelength, extension of the wave packet and temporal evolution, indicating that the simulated wave structure in both models is realistic, though the regression coefficients are larger than in the NCEP re-analysis. Larger regression coefficients translate into larger amplitudes of the waves. The overall effect of more intense synoptic-systems is a larger eddy kinetic energy, as was pointed out above. Both models also capture the northeastward propagation of the waves in the vicinity of the Andes, though the NW-SE tilts of the disturbances on the lee side are slightly overestimated, in agreement with larger eddy momentum fluxes. The orographic influence of the Andes mountains is better resolved in the high-resolution simulation for the waves emanating from the polar branch of the Pacific storm-track. A larger meridional tilt of the waves that develop downstream of the Andes mountains, as shown, produces larger eddy momentum fluxes at upper levels, which may explain the stronger and poleward shifted westerlies. This feature of the high frequency disturbances is enhanced for the high-resolution simulation, which produces westerlies, which are even stronger and displaced further poleward.

In addition, the patterns of regression coefficients suggest that, although the simulated mean baroclinicity at lower levels for both model resolutions are comparable to the observations, and even weaker in some regions, the eddy activity is stronger. The evolution of upper level synoptic disturbances reveals that the mechanism of downstream development (i.e. upstream centres that decay as new ones grow downstream maintaining the total extent of the wave packet over regions where the eddy growth rate at lower levels is weak (Orlanski and Katzfey, 1991; Solman and Menéndez, 1998) may be responsible for more active eddies in the simulations.

Many of the findings of this study, concerning the impact of the resolution, are similar to other published studies (Stratton 1999, Hasegawa *et al*., 1997; Williamson *et al*., 1995). All these studies tend to confirm that increasing resolution tends to increase the model eddy kinetic energy. Moreover, the convergence of the simulation for the extratropics is achieved around T42 (approximately 2.8° by 2.8°) and going to higher resolution continues to improve the simulation albeit with smaller changes, mainly concerning regional features. Some of the shortcomings of HadAm2b appear to be almost independent of resolution. Presumably, they may be related to the physical parameterisations.

Acknowledgements

This work has been supported by the European Commission under contract CT94-0111, the UBA Grant *X072* and the ANPCyT Grant 7-6335. The authors would like to thank Mrs. Cindy Bunton for her help during the storage of model outputs at the Hadley Centre and Dr. Rachel Stratton for preparing the eddy statistics from ERA data set. We also thanks to Dr. Isidoro Orlanski and anonymous reviewer for their comments.

References

Adler, R.F. 1971. A comparison of the general circulations of the Northern and Southern Hemispheres based on satellite, multi-channel radiance data, *Mon. Wea. Rev.* **103**, 52-60.

Berbery, E.H. and C.S. Vera, 1996. Characteristics of the southern hemisphere winter storm track with filtered and unfiltered data, *J. Atmos. Sci*. **53**, 468-481.

Boville, B.A. 1991. Sensitivity of simulated climate to model resolution, *J. Clim*. **4**, 469-485.

Boyle, J.S. 1993. Sensitivity of dynamical quantities to horizontal resolution for a climate simulation using the ECMWF (cycle 33) Model, *J. Clim*, **6**, 796-815.

Chang, E.K.M. 1993. Downstream development of baroclinic waves as inferred from regression analysis, *J. Atmos. Sci*. **50**, 2038-2053.

Gan, M.A. and V.B Rao. 1994. The influence of the Andes Cordillera on transient disturbances, *Mon. Wea. Rev.* **122**, 1141-1157.

Garreaud, R. D. and D. S. Battisti, 1999. Interannual (ENSO) and interdecadal (ENSO-like) variability in the Southern Hemisphere tropospheric circulation, *J. Clim*. **12**, 2113 – 2123.

Hasegawa, A., H.L. Tanaka, H. Hirakuchi and S. Taguchi, 1997. Comparative energetics analysis of CCM2 with different horizontal resolutions, *Clim. Dyn*. **12**, 521-532.

Hoskins, B.J. and P.J. Valdes 1990. On the existence of storm tracks. *J. Atmos. Sci*. **47**, 1854 - 1864.

Hudson D.A. and Hewitson B.C. 1997. Mid-latitude cyclones south of Africa in the GENESIS GCM, *Int. J. of Climatol*. **17**, 459-473.

Hurrell, J.W., J.J. Hack, B.A. Boville, D.L. Williamson and J.T. Kiehl, 1998. The dynamical simulation of the NCAR community climate model version 3 (CCM3), *J. Clim.*, **11**, 1207-1236.

Joubert, A.M. 1997. Simulations by the atmospheric model intercomparison project of atmospheric circulation over southern Africa, *Int. J. of Climatol*. **177**, 1129-1154.

indicar nombres de coautores

Kalnay E. **and coauthors** 1996. The NCEP/NCAR 40-year reanalysis project, *Bull. Amer. Meteor. Soc.* **77**, 437-471.

Karoly, D., D. Vincent and J. Schrage, 1998. General Circulation, In: Karoly D. and D. Vincent, (eds.), *Meteorology of the Southern Hemisphere*, American Meteorological Society. 47-88.

Katzfey J.J. and K.L. McInnes, 1996. GCM simulations of eastern Australian cutoff lows, *J. Clim.*

indicar nombres de coautores

9, 2337-2355.

Kistler R. and **Co-authors**, 2001: The NCEP-NCAR 50-year reanalysis: Monthly means CD-ROM and documentation. *Bull. Amer. Meteor. Soc*. ***82***, 247-267.

Lal, M., U. Cubasch, J. Perlwitz and J. Waszkewitz, 1997. Simulation of the Indian Monsoon climatology in ECHAM3 climate model: sensitivity to horizontal resolution*, Int. J. of Climatol.* **17**, 847-858.

Lau, K.H. and N.C. Nath 1991. Variability of the baroclinic and barotropic transient eddy forcing associated with monthly changes in middle latitude storm tracks, *J. Atmos. Sci*. **48**, 2589-2613.

Li, Z.X. and A.Carril, 1998. Transient properties of atmospheric circulation in two reanalysis datasets, Note N° 10, Institut Pierre Simon Laplace des Science de l'Environmement Global.

Lim, G.H. and J.M.Wallace, 1991. Structure and evolution of baroclinic waves as inferred from regression analysis, *J. Atmos. Sci.* **48**, 1718-1731.

Lindzen, R.S. and B. Farrell, 1980. A simple approximate result for maximum growth rate of baroclinic instabilities, *J. Atmos. Sci*. **37**, 1648-1654.

Meehl, G.A. 1998. Climate modelling. In: Karoly D. and D. Vincent (eds.), *Meteorology of the Southern Hemisphere*, American Meteorological Society, 365-410.

Orlanski, I. 1998. Poleward deflection of storm tracks, *J. Atmos. Sci*. **55**, 2577-2602.

Orlanski, I. and J.J. Katzfey, 1991. The life cycle of a cyclone wave in the Southern Hemisphere. Part I: Eddy energy budget, *J. Atmos. Sci*. **48**, 1972-1998.

Peixoto, J.P. and A.H. Oort, 1984. Physics of climate, *Review of Modern Physics*, **56**, 365-429.

Phillips, T.J., L.C. Corsetti and S.L. Grotch, 1995. The impact of horizontal resolution on moist processes in the ECMWF model, *Clim. Dyn*. **11**, 85-102.

Raphael, M. 1998. Quasi-Stationary Waves in the Southern Hemisphere: An Examination of their Simulation by the NCAR Climate System Model, with and without an Interactive Ocean, *J. Clim*. **11**, 1405-1418.

Renwick, J.A. and M. J. Revell, 1999: Blocking over the South Pacific and Rossby wave propagation. *Mon. Wea. Rev*. **127**, 2233-2247.

Simmonds, I. and K. Keay, 2000. Mean Southern Hemisphere extratropical cyclone behavior in the 40-year NCEP-NCAR Reanalysis. *J. Climate*, **13**, 873-885.

Solman, S. and C. Menéndez, 1998. Study of a cyclone wave in the Drake Passage region, *Atmósfera*, **11**, 11-28.

Solman, S. and C.Menéndez, 2002. ENSO – related variability of the Southern Hemisphere winter storm track over the eastern Pacific – Atlantic sector, *J. Atmos. Sci.* 59, 2128-2140.

Stratton, R.A. 1999. A high resolution AMIP integration using Hadley Centre model HadAm2b, *Clim. Dyn*. **15**, 9-28.

van Loon, H. and R. Jenne 1972. The zonal harmonic standing waves in the Southern Hemisphere,

J. Geophys. Res. **77**, 992-1003.

Wallace J.M., Lim G.H. and Blackmon M.L. 1988. Relationship between cyclone tracks, anticyclone tracks and baroclinic waveguides, *J. Atmos. Sci*. **45**, 439-462.